



UNIVERSITI PUTRA MALAYSIA

***INVESTIGATION OF DIFFERENT CONFIGURATIONS FOR SINGLE AND
DOUBLE SPACING MULTI-WAVELENGTH BRILLOUIN-RAMAN FIBER
LASER***

GHAZALEH MAMDOOHI

FK 2014 153



**INVESTIGATION OF DIFFERENT CONFIGURATIONS FOR SINGLE
AND DOUBLE SPACING MULTI-WAVELENGTH BRILLOUIN-
RAMAN FIBER LASER**

By

GHAZALEH MAMDOOHI

**Thesis Submitted to the School of Graduate Studies, Universiti Putra Malaysia,
in Fulfillment of the Requirements for the Degree of Doctor of Philosophy**

December 2014



© COP YRIGHT UPM

COPYRIGHT

All materials contained within the thesis, including without limitation text, logos, icons, photographs and all other artwork, is copyright material of Universiti Putra Malaysia unless otherwise stated. Use may be made of any material contained within the thesis for non-commercial purposes from the copyright holder. Commercial use of material may only be made with the express, prior, written permission of Universiti Putra Malaysia.

Copyright © Universiti Putra Malaysia



© COPYRIGHT UPM

*This thesis is dedicated to:
my dearest patient husband,
and my beloved parents*



© COPYRIGHT UPM

Abstract of thesis presented to the Senate of Universiti Putra Malaysia in fulfillment of the requirement for the degree of Doctor of Philosophy

INVESTIGATION OF DIFFERENT CONFIGURATIONS FOR SINGLE AND DOUBLE SPACING MULTI-WAVELENGTH BRILLOUIN-RAMAN FIBER LASER

By

GHAZALEH MAMDOOHI

December 2014

Chairman: Mohd Adzir bin Mahdi, PhD
Faculty: Engineering

The work in this thesis focuses on generation of multi-wavelength Brillouin-Raman fiber laser (MBRFL) with single and double frequency Brillouin spacing shift. Three main configurations have been proposed to accomplish this aim. These are achieved based on the stimulated Brillouin scattering (SBS), stimulated Raman scattering (SRS), and stimulated Rayleigh scattering (SRLS). In all architectures, dispersion compensating fiber (DCF) is utilized as a nonlinear Brillouin-Raman gain medium. Firstly, a new MBRFL utilizing enhanced nonlinear amplifying fiber loop (NAFL) design is proposed and demonstrated to produce adjustable 10 and 20 GHz wavelength spacing. We developed a detailed theoretical analysis, which represents a good foundation on which operation of MBRFL with 10 and 20 GHz spacing is satisfied. By proper adjustments of splitting ratio, the wavelength interval can be adjusted, thus improving the laser performance. Utilizing 50/50 coupler offers 443 flat amplitude channels with 10 GHz spacing and 16.5 dB average Stokes optical signal-to-noise ratio (S-OSNR). On the other hand, 1/99 coupler is desirable for multiple Stokes combs with 20 GHz spacing in which 221 lasing lines with an average 25 dB S-OSNR are generated. The employment of a mirror at the end of this cavity, which is dubbed as the nonlinear amplifying loop mirror (NALM) design is responsible for initiation of lower threshold for SBS effect that leads to the excellent results. A total of 28 channels with 10 GHz spacing and an average 17 dB S-OSNR are achieved when the Raman pump power (RPP) is fixed at only 300 mW. This is the most efficient 10 GHz MBRFL reported at very low RPP through a simple configuration. The second configuration is proposed to generate a MBRFL with 20 GHz spacing via forward pumping scheme. The setup is arranged in a linear cavity by employing 7.2 and 11 km DCF in addition to a 30 cm Bismuth oxide erbium-doped fiber (Bi-EDF). It is found that incorporating 11 km DCF with Bi-EDF results in multiple Brillouin Stokes signals with outstanding OSNR. In this case, a total of 186 Brillouin Stokes combs with -13.5 dBm Stokes peak power (SPP) and an average 28 dB S-OSNR are produced. These results are achieved when Brillouin pump (BP) power of -2.6 dBm, BP wavelength of 1545 nm, and RPP of 900 mW are injected into the cavity. However, characteristics improvement of MBRFL with 20 GHz spacing in terms of channels count, SPP, and wavelength operation is

another aim of this work which is successfully accomplished by introducing the third configuration. In this structure, incorporation of Raman pump source with a set of couplers with various ratios leads to different Brillouin Stokes lines features. The optimization of multi-wavelength laser operation is done with proper adjustments of coupling ratio, BP wavelength, BP power, and RPP. The results demonstrate that the best S-OSNR performance is satisfied at coupling ratio of 50/50. When setting the RPP to 1000 mW, 212 flat amplitude Stokes lines with -10 dBm SPP and an average 27.5 dB S-OSNR are achieved. In this case, the BP power and its corresponding wavelength are set at -2.6 dBm and 1543 nm respectively. Moreover, this configuration reveals the highest peak power discrepancy between odd- and even-order Stokes lines (22.5 dB) in comparison with other configurations with 20 GHz spacing.



Abstrak tesis yang dikemukakan kepada Senat Universiti Putra Malaysia sebagai memenuhi keperluan untuk ijazah Doktor Falsafah

**SIASATAN TERHADAP KONFIGURASI-KONFIGURASI BERBEZA
UNTUK TUNGGAL DAN BERKEMBAR PADA LASER GENTIAN
BRILLOUIN-RAMAN BERBILANG SALURAN**

Oleh

GHAZALEH MAMDOOHI

Decimber 2014

Pengerusi: Mohd Adzir bin Mahdi, PhD
Fakulti: Kejuruteaan

Kerja penyelidikan ini memfokus kepada penghasilan laser gentian Brillouin-Raman berbilang saluran (MBRFL) dengan anjakan selang Brillouin berfrekuensi tunggal dan berkembar. Tiga konfigurasi utama telah disyorkan dalam kerja penyelidikan ini. Ianya dicapai berdasarkan penyerakan Brillouin terangsang (SBS), penyerakan Raman terangsang (SRS), dan penyerakan Rayleigh terangsang (SRLS). Di dalam semua binaan, gentian gantian penyebaran (DCF) digunakan sebagai sebuah media pengganda Brillouin-Raman tidak lurus. Pertamanya, sebuah MBRFL yang baru menggunakan rekaan gelung gandaan tidak lurus (NAFL) termaju telah disyorkan dan didemonstrasikan untuk menghasilkan selang saluran boleh-ubah iaitu 10 dan 20 GHz. Kami juga telah membangunkan suatu analisis teori yang terperinci, di mana ianya adalah suatu penemuan yang bagus, yang mana operasi MBRFL dengan selang 10 dan 20 GHz adalah memuaskan. Dengan perubahan yang betul terhadap nisbah pecahan, selang saluran boleh diubah, seterusnya meningkatkan prestasi laser. Menggunakan pengganding 50/50 menawarkan selang-selang amplitud rata sejumlah 443 garisan laser dengan 10 GHz dan hampir kepada nilai 16.5 dB untuk nisbah isyarat-kepada-kebisingan optik Stokes (S-OSNR). Selain daripada itu, pengganding 1/99 diperlukan untuk sesikat Stokes berbilang dengan selang 20 GHz, di mana bilangan saluran sejumlah 221 dengan S-OSNR bernilai 25 dB telah dihasilkan. Penggunaan cermin pada hujung kaviti ini di gelar sebagai rekaan cermin gelung gandaan tidak lurus (NALM) dan bertanggungjawab untuk penghasilan nilai ambang yang lebih rendah untuk kesan SBS yang membawa kepada keputusan yang bagus. Sejumlah 28 saluran dengan selang 10 GHz dan purata S-OSNR bernilai 17 dB telah dicapai apabila kuasa pam Raman (RPP) ditetapkan pada 300 mW sahaja. Ia merupakan laporan MBRFL untuk 10 GHz yang paling efisien pada RPP yang paling rendah berdasarkan kepada konfigurasi yang ringkas. Konfigurasi kedua mensyorkan penghasilan suatu MBRFL dengan selang 20 GHz melalui skim pengepaman hadapan. Penyediaan ini disusun dalam kaviti lurus dengan menggunakan DCF yang panjangnya 7.2 dan 11 km, dengan penambahan gentian erbium-terdop Bismuth teroksida (Bi-EDF) yang panjangnya 30 cm. Menggunakan Bi-EDF berserta DCF yang panjangnya 11 km, didapati isyarat Stokes Brillouin berbilang dengan OSNR yang bagus terhasil. Dalam kes ini,

sejumlah 186 sesikat Stokes Brillouin dengan kuasa puncak Stokes (SPP) bernilai -13.5 dBm dan S-OSNR bernilai 28 dB telah dihasilkan. Keputusan ini dicapai apabila kuasa pam Brillouin (BP) adalah -2.6 dBm, saluran BP adalah 1545 nm, dan RPP adalah 900 mW dimasukkan ke dalam kaviti. Akan tetapi, peningkatan ciri MBRFL dengan selang 20 GHz dari segi pengiraan saluran, SPP, dan operasi saluran adalah matlamat lain dalam kerja penyelidikan ini, yang mana telah berjaya dicapai dengan memperkenalkan konfigurasi ketiga. Dalam struktur ini, kemasukan sumber pam Raman dengan set pengganding pelbagai nisbah menunjukkan kepada sifat garisan Stokes Brillouin yang berbeza. Pengoptimuman operasi laser berbilang saluran dapat dicapai dengan pengubahan nisbah penggandingan, saluran BP, kuasa BP dan RPP. Keputusan ini menyatakan bahawa prestasi S-OSNR terbaik telah dicapai pada nisbah penggandingan 50/50. Apabila RPP ditetapkan pada 1000 mW, 212 garisan Stokes amplitud rata dengan SPP bernilai -10 dBm dan purata S-OSNR bernilai 27.5 dB telah diperolehi. Dalam kes ini, kuasa BP ditetapkan kepada -2.6 dBm, manakala panjang gelombang saluran BP ditetapkan kepada 1543 nm. Selain itu, konfigurasi ini mendedahkan bahawa perbezaan kuasa puncak tertinggi di antara garisan Stokes pada susunan ganjil dan genap adalah bernilai 22.5 dB dalam perbandingan dengan konfigurasi lain dengan selang 20 GHz.

ACKNOWLEDGEMENTS

All grace and thanks belongs to Almighty Allah for giving me the strength, courage, and determination for completing this work, Alhamdulillah.

I would like to express my sincere gratitude to my supervisor Prof. Mohd Adzir bin Mahdi for his guidance, advice, and encouragement in the completion of this study. His professional review helped me to further improve the thesis.

Special thanks dedicated to my supervisory committee member, Dr. Makhfudzah Bt. Mokhtar, Dr. Hanif Yaacob, and Dr. Abdul Rahman Sarmani for their motivations and encouragements.

I would like to express my deepest gratitude to my beloved husband, Behnam Kheradmand, for his endless support during 7 years studying beside him.

Last but not least I am proud and grateful to my beloved parents and my parents in law for being so helpful and supportive through my studies.

APPROVAL

I certify that a Thesis Examination Committee has met on 18th December 2014 to conduct the final examination of Ghazaleh Mamdoohi on her thesis entitled “Investigation of different configurations for single and double spacing multi-wavelength Brillouin–Raman fiber laser” in accordance with the Universities and University Colleges Act 1971 and the Constitution of the Universiti Putra Malaysia [P.U.(A) 106] 15 March 1998. The Committee recommends that the student be awarded the Doctor of Philosophy.

Members of the Thesis Examination Committee were as follows:

Nor Kamariah bt. Noordin, PhD

Professor
Faculty of Engineering
Universiti Putra Malaysia
(Chairman)

Salasiah bt. Hitam, PhD

Faculty of Engineering
Universiti Putra Malaysia
(Internal Examiner)

Md Zaini bin Jamaludin, PhD

Professor
Faculty of Engineering
Universiti Tenaga Nasional (UNITEN)
(External Examiner)

Meil Grogory Raphael Broderick, PhD

Professor
Faculty of Physics
University of Auckland
(External Examiner)

NORITAH OMAR, PhD.

Assoc. Professor and Deputy Dean
School of Graduate Studies
Universiti Putra Malaysia
Date:

This thesis was submitted to the Senate of Universiti Putra Malaysia and has been accepted as fulfillment of the requirement for the degree of Doctor of Philosophy. The members of the Supervisory Committee were as follows:

Mohd Adzir bin Mahdi, PhD

Professor
Faculty of Engineering
Universiti Putra Malaysia
(Chairman)

Makhfudzah Bt Mokhtar, PhD

Senior Lecturer
Faculty of Engineering
Universiti Putra Malaysia
(Member)

Mohd Hanif Yaacob, PhD

Senior Lecturer
Faculty of Engineering
Universiti Putra Malaysia
(Member)

Abdul Rahman Sarmani, PhD

Senior Lecturer
Faculty of Science
Universiti Putra Malaysia
(Member)

BUJANG BIN KIM HUAT, PhD

Professor and Dean
School of Graduate Studies
Universiti Putra Malaysia

Date:

Declaration by graduate student

I hereby confirm that:

- this thesis is my original work;
- quotations, illustrations and citations have been duly referenced;
- this thesis has not been submitted previously or concurrently for any other degree at any other institutions;
- intellectual property from the thesis and copyright of thesis are fully-owned by Universiti Putra Malaysia, as according to the Universiti Putra Malaysia (Research) Rules 2012;
- written permission must be obtained from supervisor and the office of Deputy Vice-Chancellor (Research and Innovation) before thesis is published (in the form of written, printed or in electronic form) including books, journals, modules, proceedings, popular writings, seminar papers, manuscripts, posters, reports, lecture notes, learning modules or any other materials as stated in the Universiti Putra Malaysia (Research) Rules 2012;
- there is no plagiarism or data falsification/fabrication in the thesis, and scholarly integrity is upheld as according to the Universiti Putra Malaysia (Graduate Studies) Rules 2003 (Revision 2012-2013) and the Universiti Putra Malaysia (Research) Rules 2012. The thesis has undergone plagiarism detection software.

Signature: _____

Date: _____

Name and Matric No.: Ghazaleh Mamdoohi, GS29922

Declaration by Members of Supervisory Committee

This is to confirm that:

- the research conducted and the writing of this thesis was under our supervision;
- supervision responsibilities as stated in the Universiti Putra Malaysia (Graduate Studies) Rules 2003 (Revision 2012-2013) are adhered to.

Signature: _____
Name of
Chairman of
Supervisory
Committee: _____

Signature: _____
Name of
Chairman of
Supervisory
Committee: _____

Signature: _____
Name of
Chairman of
Supervisory
Committee: _____

Signature: _____
Name of
Chairman of
Supervisory
Committee: _____

TABLE OF CONTENTS

ABSTRACT	Page
ABSTRAK	i
ACKNOWLEDGEMENTS	iii
APPROVAL	v
LIST OF TABLES	vi
LIST OF FIGURES	xiii
LIST OF ABBREVIATIONS	xiv
	xviii

CHAPTER

1	INTRODUCTION	1
	1.1 Introduction	1
	1.2 Motivation	2
	1.3 Problem Statements	3
	1.4 Objectives of This Research Work	3
	1.5 Scope of Research Work	4
	1.6 Research Methodology	5
	1.7 Thesis Overview	7
2	LITERATURE REVIEW	9
	2.1 Introduction	9
	2.2 Description of Nonlinear Effects in Optical Fiber	9
	2.2.1 Nonlinear Refractive Index Effects	10
	2.2.1.1 Self-Phase Modulation	11
	2.2.1.2 Cross-Phase Modulation	11
	2.2.1.3 Four-Wave Mixing	12
	2.2.2 Inelastic Scattering Effects	12
	2.2.2.1 Stimulated Brillouin Scattering	12
	2.2.2.2 Stimulated Raman Scattering	13
	2.3 Single-Pump Raman Amplification	15
	2.3.1 Forward Pumping	16
	2.3.2 Backward Pumping	16
	2.3.3 Signal Gain	16
	2.4 Nonlinear Fiber Devices	17
	2.4.1 Sagnac Interferometers	17
	2.5 Nonlinear Optical Loop Mirror	18
	2.5.1 Nonlinear Transmission	19
	2.6 Basic Overview on Generation of Multiple Lasing Wavelengths	21
	2.6.1 Principle Operation of MBRFLs Generation	22
	2.7 Review on Multi-wavelength Brillouin-Raman Fiber Lasers	23
	2.8 Summary	28
3	DEVELOPMENT SIMPLE CONFIGURATIONS FOR GENERATION MBRFL WITH 10 AND 20 GHz SPACING	29

3.1	Introduction	29
3.2	Experimental Setup for Generation MBRFL with Adjustable Wavelength Spacing Utilizing Enhanced NAFL Design	30
3.3	Principle Theory of NALM	31
3.3.1	Analytical Model	33
3.3.1.1	Development of Transmitted and Reflected Output Powers	34
3.3.1.2	Development of Nonlinear Phase Shift	37
3.3.1.3	Analysis of Nonlinear Output Power and Phase Shift Characteristics	38
3.3.1.4	Numerical Result for Nonlinear Phase Shift of Output Signal	40
3.4	Principle Operation of MBRFL Utilizing NAFL	41
3.5	Experimental Results and Discussions	43
3.5.1	Effect of Different Coupling Ratios on Peak Power Discrepancy between Odd and Even Order Brillouin Stokes Lines	43
3.5.2	Effect of Multiple Interference between Beating Spectra for Generation MBRFL	44
3.5.3	Generation of MBRFL with 10 and 20 GHz Spacing	45
3.5.4	Effect of RPP on MBRFL Spectrum OSNR	47
3.5.5	Effect of RPP and BP Power on Number of Stokes Lines	50
3.5.6	Effect of Coupling Ratios on MBRFL Bandwidth	52
3.5.6.1	ASE Spectrum of MBRFL for Different Coupling Ratios	52
3.5.6.2	Effect of Different BP Wavelengths on Number of Lasing Lines	53
3.6	Generation MBRFL with 10 GHz Spacing Utilizing Enhanced NALM Design	55
3.6.1	Laser Structure and Operation Principle	55
3.7	Experimental Results and Discussions	56
3.7.1	Effect of Different Coupling Ratios on Transmitted and Reflected Powers	56
3.7.2	Effect of RPP on S-OSNR	58
3.7.3	Effect of BP Power on Number of Channels	59
3.7.4	Tunability of 10 GHz Spacing MBRFL	60
3.8	Summary	61

4 20 GHz SPACING MULTI-WAVELENGTH GENERATION OF BRILLOUIN-RAMAN FIBER LASER IN A LINEAR CAVITY 62

4.1	Introduction	62
4.2	Experimental Setup for 20 GHz Spacing MBRFL through FWP Scheme	62

4.3	Principle Operation of 20 GHz MBRFL Generation	63
4.4	Experimental Results and Discussions	64
4.4.1	ASE Spectra for Different Gain Media Schemes	64
4.4.2	Effect of Residual RPP on Bi-EDF Amplification	65
4.4.3	Effect of RPP on Number of Lasing Lines	66
4.4.4	Effect of Different BP Power on SLC at Various RPP Values	69
4.4.5	Effect of BP Wavelength on Number of Lasing Lines	70
4.4.6	Effect of BP Wavelength on S-OSNR	74
4.4.7	Effect of RPP on MBRFL Spectrum OSNR	75
4.4.8	Tuning Range of MBRFL for Different Gain Media Arrangements	77
4.5	Experimental Setup for Variation Effects of Raman Pump Power Distribution on MBRFL	79
4.6	Results and Discussions	80
4.6.1	Investigation of ASE Spectra of Different Pumping Schemes through their Raman Gain Distribution Analysis	80
4.6.2	Effects of Different Pumping Ratios on MBRFL Spectrum	82
4.6.3	Effect of Different Coupling Ratios and RPP Values on MBRFL Spectrum OSNR	86
4.6.4	Effect of Different RPP and Pumping Schemes on Brillouin Stokes Count	87
4.6.5	Effect of BP Wavelength on SLC at Various Pumping Ratios	89
4.6.6	Effect of BP Wavelength and Pumping Schemes on MBRFL OSNR	90
4.7	Summary	93
5	CONCLUSION AND FURTHER WORKS	94
5.1	Introduction	94
5.2	Conclusion	94
5.3	Contribution	95
5.4	Further Works and Suggestion	96
	REFERENCES	98
	APPENDIX	103
	BIODATA OF STUDENT	105
	LIST OF PUBLICATIONS	106

LIST OF TABLES

Table	Page
2.1 Summary of the previous works that cover MBRFL.	27
5.1 Summary of the previous works and experimental findings at this thesis that cover MBRFL generated in a linear cavity.	97



LIST OF FIGURES

Figure	Page
1.1: Scope of doctoral research.	5
1.2: Research methodology flow-chart.	7
2.1: Schematic of the nonlinear effects in fiber optics.	10
2.2: Schematic plot of the SBS generation in optical fibers.	13
2.3: Schematic of the energy levels of a molecule involved during stimulated Raman scattering [52].	14
2.4: Schematic of an all-fiber Sagnac interferometer.	18
2.5: Schematic illustration of (a) NOLM and (b) NALM by the SPM effect.	19
2.6: Schematic illustration of an all-fiber Sagnac interferometer acting as a NOLM. A_{in} , A_f , A_b , A_f' , A_b' , A_t , and A_r : Amplitudes for the propagating beams where indexes f and b indicate partial input beams in forward-(CW) and backward-(CCW) respectively, subscript in indicates input beam and the superscript symbols signify input beams after one round trip. Moreover, signals with indexes t and r represent the transmitted and reflected output waves respectively.	19
2.7: Transmitted power as a function of incident power for two values of α , showing the nonlinear response of an all-fiber Sagnac interferometer [56].	21
2.8: Pioneer design of proposed MBRFL in [17].	23
2.9: The proposed ring and linear cavity MBRFL and their output spectrum shown in (a), (b), and (c) are reported in [20], [21], and [20] respectively.	24
2.10: MBRFL architecture in (a) full open and (b) half open linear cavity at [23] and [27] respectively.	25
3.1: MBRFL design by utilizing an enhanced NAFL. C_1 , C_3 , and C_4 : Circulators with indexes 1, 3, and 4 that relate to their corresponding connections to the VOC ports as demonstrated in the dashed boxes. P_1 , P_2 , P_t , and P_r : Signal powers where indexes 1 and 2 indicate partial input beam and indexes t and r represent the transmitted and reflected output power respectively.	31
3.2: Simplified diagram of the laser architecture described in Figure 3.1. The VOC is adjusted to divide the input signal coupling at port 3/4 according to several ratios of 1/99, 5/95, 20/80, 30/70, 50/50, 70/30, 80/20, 95/5, and 99/1. A_{in} , A_1 , A_2 , A_1' , A_2' , A_t , and A_r : Amplitudes for the signal beams where index in indicates an input beam, the superscript symbols signify an input beams that experience Raman amplification. Indexes 1 and 2 indicate partial input beam and subscripts t and r represent the transmitted and reflected output signals respectively.	31
3.3: The induced phase shift of the output signal as a function of coupling ratio (RPP=1000 mW, BP=3 mW (5 dBm), L=7.2 km).	41
3.4: Peak power difference between odd- and even-order BSL measured at port 1 and 2 of the different coupler as a function of coupling ratio (RPP= 1000 mW, BP wavelength= 1555 nm, BP power =5 dBm).	44
3.5: Spectra of the beating signals measured at C_3 and C_4 for 70/30 coupler. The black and red lines show the output spectra at OSA1 and OSA2 respectively (RPP= 1000 mW, BP wavelength= 1555 nm, BP power =5 dBm). TBS1, TBS2: Transmitted Brillouin signals along port 3 and 4 in that order, the indexes 1 and	

- 2 for all signals represent the partial signals generated by CW and CCW correspondingly. 45
- 3.6: Spectra of the traveling Stokes signals measured at C_3 and C_4 for (a) 10 GHz and (b) 20 GHz spacing. The black and red lines show the output spectra at OSA1 and OSA2 respectively (RPP= 1000 mW, BP wavelength= 1555 nm, BP power =5 dBm). 46
- 3.7: Average S-OSNR values versus RPP variation at optimum coupling ratios (BP power =5 dBm, BP wavelength=1555 nm). 47
- 3.8: Stokes spectral broadening with increasing RPP for different coupling ratios (BP power =5 dBm, BP wavelength=1555 nm). 49
- 3.9: Number of channels versus RPP for coupling ratio 1/99, 50/50, and 99/1. The BP wavelength is maintained at 1555 nm and the BP power is set to -2.6, 1.2, and 5 dBm. 51
- 3.10: The spectra for 1/99, 50/50, and 99/1 dB coupler obtained when the RPP is fixed at 700 mW, while the BP power and its corresponding wavelength are set at 5 dBm and 1555 nm respectively. 51
- 3.11: Illustration of multi-wavelength bandwidth spectrum for 50/50 couplers (BP wavelength=1555 nm, BP power=-2.6 dBm, RPP =1000 mW). For clarification, the measurement on number of Stokes lines and an average S-OSNR is also elucidated. 52
- 3.12: ASE spectra for 1/99 and 50/50 dB couplers when the RPP is set at 1000 mW and the BP signal is switched off. 53
- 3.13: Variations of multi-wavelength bandwidth and number of channels by increasing the BP wavelengths. The RPP and BP power are fixed at 1000 mW and -2.6 dBm, respectively, for coupling ratios 1/99 and 50/50. 54
- 3.14: Spectra of MBRFL with 10 GHz (50/50) and 20 GHz (1/99) spacing and insets are the enlarged view of the BSL at 50/50 and 1/99 couplers. (RPP = 1000 mW, BP power = -2.6 dBm, BP wavelength = 1540 nm). 54
- 3.15: Experimental setup for a MBRFL utilizing an enhanced NALM. The mirror (M) is utilized in the entire assessment, but the characterization of transmitted and reflected beams at port 2 and 1 of the VOC respectively are carried out without the mirror. 55
- 3.16: (a) Output power flow of the NALM without mirror. The solid lines show the experimental results, while the dashed line represents the transmitted power calculated by Equation (3.22). The number of channels (with mirror) against the coupling ratio at port P_3/P_4 is shown in (b) (BP power =5 dBm, BP wavelength =1555 nm, RPP = 300 mW). 57
- 3.17: Output spectra of MBRFL at 200, 300, and 500 mW of RPP (with mirror, CR = 99/1, BP power =5 dBm, BP wavelength =1555 nm). 59
- 3.18: Multi-wavelength output spectra when the BP power is set at -2.6 and 5dBm, the red spectral profile was taken from Figure 3.17 for visual depiction (with mirror, CR = 99/1, BP wavelength =1555 nm, RPP = 300 mW). The inset shows the free running lasing mode profile obtained when the BP power is switched-off. 60
- 3.19: Wavelength tuning at 300 mW RPP and -2.6 dBm BP power. The labels illustrate the number of BSL. 61
- 4.1: Experimental setup for a MBRFL where the hybrid DCF-Bi-EDF gain media is shown in the blue-dashed box. 63

- 4.2: ASE spectra of MBRFL at different gain media configurations when the BP signal is switched off and the RPP is set to 800 and 1000 mW. 64
- 4.3: The amplification of BP signal through Bi-EDF when is pumped by 62 and 98 mW RPP. The results are achieved when the DCF is removed from the setup and the BP power is set at 5 dBm. 65
- 4.4: Number of output channels versus RPP variation for different fiber schemes, the BP power and its corresponding wavelength are fixed at 5 dBm and 1555 nm respectively. 67
- 4.5: Illustrations of multi-wavelength lasing spectra at different RPP values for (a) 7.2 km DCF, (b) 7.2 km DCF with Bi-EDF, (c) 11 km DCF, and (d) 11 km DCF with Bi-EDF schemes. The magnified views are presented in graphs (a1), (b1), (c1), and (d1) where their colors correspond to the relevant RPP values (BP wavelength = 1555 nm, BP power = 5 dBm). 68
- 4.6: Evolution of number of Stokes lines versus the RPP for various arrangements, the BP wavelength is maintained at 1555 nm and the BP power is set to 5, 1.2, and -2.6 dBm. 69
- 4.7: Variations of Stokes count by increasing the BP wavelengths. The RPP and BP powers are fixed at 1000 mW and -2.6 dBm, respectively for all arrangements. 71
- 4.8: Demonstrations of lasing comb spectra of different configurations at (a) 1550, (b) 1555, and (c) 1565 nm BP wavelengths respectively (BP power=-2.6 dBm and RPP= 1000 mW). 73
- 4.9: (a) S-OSNR variations against the BP wavelength increment (RPP and BP power are fixed at 1000 mW and -2.6 dBm respectively). 74
- 4.10: Illustrations of total SLC and S-OSNR variations against the RPP increment. The BP wavelengths are set at 1545 nm, 1555 nm, and 1565 nm in (a), (b), and (c) respectively while the BP power is maintained at -2.6 dBm. 76
- 4.11: Tunability of the MBRFL for different structures, the DCF length is extended from (a) 7.2 km to (b) 11 km and by employing Bi-EDF to the corresponding DCF lengths as shown in (c) and (d) respectively (RPP = 1000 mW and BP power = -2.6 dBm). 78
- 4.12: Output spectrum of 20 GHz MBRFL utilizing 11 km DCF with 30 cm Bi-EDF whilst the RPP, BP wavelength, and BP power are chosen at 900 mW, 1545 nm, and -2.6 dBm, respectively. The enlarge view is illustrated as the inset graph. 79
- 4.13: Schematic diagram of a MBRFL where the dashed boxes indicate the pumping arrangements. In the BiDP, the couplers utilized in forward/backward directions are 5/95, 10/90, 20/80, 30/70, 50/50, 70/30, 80/20, 90/10, and 95/5. In addition, no couplers are included for 100% FWP and 100% BWP as shown in the insets. 80
- 4.14: ASE spectra at different coupling ratios when the RPP is set at 1000 mW and the BP signal is switched off. The CR labels are arranged from top to bottom level in descending order of output power values. 81
- 4.15:(a) Spectra output of MBRFLs, (b) the magnified views of spectral features at different RPP couplings namely, 100% BWP, 20/80, 50/50, 90/10, and 100% FWP and (c) illustration of 10 and 20 GHz spacing MBRFL spectra for BWP and 90/10 coupler as an example. For simplification, other CRs results are not shown (RPP and BP power are fixed at 1000 mW and 5 dBm, respectively, while the BP wavelength is set at 1555 nm). 84

- 4.16: Peak power difference between odd- and even-order BSL as a fraction of RPP toward FWP (r_f) (RPP= 1000 mW, BP wavelength= 1555 nm, BP power =5 dBm). 86
- 4.17: (a) Evolutions of S-OSNR against RPP increment, the CR labels are arranged from top to bottom levels in descending-order of S-OSNR values and (b) illustration of the spectral broadening effect on S-OSNR reduction against the RPP increment from 800 to 1000 mW when 100% FWP scheme is chosen (BP wavelength= 1555 nm, BP power = 5 dBm). 87
- 4.18: (a) Number of output channels versus RPP increment at different CRs, (b) threshold power as a function of r_f (RPP = 1 W, BP power = 5 dBm, BP wavelength=1555 nm). 88
- 4.19: The dependency of lasing lines count on BP wavelength for various pumping ratios (RPP=1000 mW, BP wavelength=-2.6 dBm). 90
- 4.20:(a) Evolutions of S-OSNR and SLC as a function of BP wavelength, (b) variation of Stokes peak power against the BP wavelength increment at different pumping ratios. RPP and BP power are fixed at their optimized values which are known as 1 W and -2.6 dBm respectively. 91
- 4.21: Spectrum of MBRFL together with its enlarged view when the CR is set at 50/50 (RPP=1000 mW, BP power= -2.6 dBm, BP wavelength =1543 nm). 92

LIST OF ABBREVIATIONS

AGC	Asiah Glass Company
Al ₂ O ₃	Alumina
ASE	Amplified Spontaneous Emission
BWP	Backward Pumping
Bi-EDF	Bismuth Oxide Erbium-Doped Fiber
BiDP	Bidirectional Pumping
Bi ₂ O ₃	Bismuth Oxide
BFL	Brillouin Fiber Laser
BP	Brillouin Pump
BS	Brillouin Stokes
BSL	Brillouin Stokes Lines
BEFL	Brillouin-Erbium Fiber Laser
BRFL	Brillouin-Raman Fiber Laser
C	Circulator
CW	Clockwise
CCW	Counter-Clockwise
CR	Coupling Ratio
DWDM	Dense Wavelength Division Multiplexing
DCF	Dispersion Compensating Fiber
DSF	Dispersion Shifted Fiber
EDF	Erbium-Doped Fiber
EDFL	Erbium-Doped Fiber Laser
EDFA	Erbium-Doped Fiber Amplifier
Er ⁺³	Erbium
1 st BSL	First Brillouin Stokes Line
FWP	Forward Pumping
FWM	Four-Wave Mixing
GeO ₂	Germanium Oxide
HNLF	Highly Nonlinear Fiber
I	Isolator
La	Lanthanum
LEAF	Large Effective Area Fiber
M	Mirror
MBEFL	Multi-wavelength Brillouin-Erbium Fiber Laser
MFL	Multi-wavelength Fiber Laser
MBRFL	Multi-wavelength Brillouin-Raman Fiber Laser
MBSS	Multiple Brillouin Stokes Signals
NAFL	Nonlinear Amplifying Fiber Loop
NALM	Nonlinear Amplifying Loop Mirror
NOLM	Nonlinear Optical Loop Mirror
NPR	Nonlinear Polarization Rotation
OA	Optical Amplifier
OPM	Optical Power Meter
OSNR	Optical Signal-to-Noise Ratio
OSA	Optical Spectrum Analyzer
RFL	Raman Fiber Laser

RPG	Raman Peak Gain
RPP	Raman Pump Power
RPU	Raman Pump Unit
RLBS	Rayleigh Backscattering
2 nd BSL	Second Brillouin Stokes Line
SiO ₂	Silicon Oxide
Si-EDF	Silicon oxide Erbium-Doped Fiber
SPM	Self-Phase Modulation
SMF	Single Mode Fiber
SBS	Stimulated Brillouin Scattering
SRS	Stimulated Raman Scattering
SRLS	Stimulated Rayleigh Scattering
SLC	Stokes Lines Count
S-OSNR	Stokes-Optical Signal-to-Noise Ratio
SPP	Stokes Peak Power
TLS	Tunable Laser Source
WDM	Wavelength Division Multiplexing
WSC	Wavelength Selective Coupler
XPM	Cross-Phase Modulation
YFL	Ytterbium Fiber Laser



© COP YRIGHT UPM

CHAPTER ONE

INTRODUCTION

1.1 Introduction

There is currently an increasing demand for transmission bandwidth used for dense wavelength-division-multiplexing (DWDM) optical communication systems as resulted from the remarkable advancement both in the data traffic and the internet [1-2]. DWDM has a potential transmission system with large number of closely spaced channels through optical fiber. In addition, employment of optical amplifiers for regenerating the multi-channel light wave without requiring to demultiplexing of individual channels makes a revolution in multi-wavelength optical system designs. This makes a demand for multi-wavelength light source. In order to fulfill such a demand, using the multi-channel laser source has turned into a noticeable and conceivable solution. Multi-wavelength fiber lasers are highly desirable for the cost and size reduction, improvement of system integration and their compatibility with optical communication networks. Researchers have focused their efforts on producing a multi-wavelength fiber laser (MFL) which is able to generate a higher number of channels with precise wavelength spacing between them. In the past few years, generating multi-wavelength based on nonlinear effects are one of the attractive approaches which were mostly designed in a single or hybrid technology. The single configuration means that only a single-technology has been deployed for this purpose such as the ones based on Brillouin fiber laser (BFL) [3-4], erbium-doped fiber laser (EDFL) [5-6], Raman fiber laser (RFL) [7-8], ytterbium fiber laser (YFL) [9], and others. However, this type of BFL suffers from a limitation in output power due to the small coefficient of the Brillouin gain. Moreover, the EDFL or RFL have some drawbacks, mainly resulting from few laser Stokes line count (SLC) and non-flattened laser Stokes spectra. These features have forced the researchers to explore the hybrid technology. Hybrid-gain configuration is another nonlinear-based multi-wavelength fiber laser which is more attractive due to its ability to generate more multi-wavelength laser. This type of configuration combines Brillouin and other gains for generating multiple wavelengths. Brillouin-Erbium fiber laser (BEFL) in ring and linear cavity have attracted many interests [10-14]. The BEFL operation is also extremely sensitive to resonance detuning between the pump laser frequency and the Brillouin cavity mode [12, 15]. However, the homogeneous nature of its gain medium limits the bandwidth and amplitude envelope profiles of the output multi-wavelength Brillouin-Erbium fiber laser (MBEFL) comb spectrum [16]. Since the number of wavelengths that can be generated in a fiber laser is critical as it is directly proportional to the transmission system capacity. Hence, a new configuration of hybrid multi-wavelength Brillouin-Raman fiber laser (MBRFL) has been regarded as a potential and prosperous solution with several important advantages. These include stable multi-wavelength operation at room temperature and the extremely broad workable wavelength band nearly without limitation. This technique was first proposed by B. Min et al. at 2001 [17] in which the narrow linewidth Brillouin gain is integrated with broad bandwidth Raman gain to generate hundreds of channels. Later on K.D. Park et al. [18-19] have studied the dynamic and threshold features of Brillouin Stokes lines (BSL) generation in Raman

fiber amplifier. Multiple-wavelength Brillouin-Raman fiber lasers having ring and linear cavity configurations have been demonstrated in [20-21]. These two studies used highly nonlinear fiber (HNLF) and dispersion shifted fiber (DSF) as a Brillouin-Raman gain medium which represent 20 and 75 Stokes lines as well as the roughly 10.5 GHz spacing for both configurations correspondingly. A. K. Zamzuri et al. recommended architectures for MBRFL which employ two feedback mirrors at the both ends of the cavities [22-23]. Moreover, they have studied the contribution of Rayleigh scattering on Brillouin comb line generation and the effect of spectral broadening on Stokes-optical signal-to-noise ratio (S-OSNR) [24-26]. Another MBRFL is also proposed by Wu et al. [27] which is performed in a half-open cavity and capable of creating uniform Stokes combs with 210 channels. Furthermore, Sonee Shargh et al. [28] have demonstrated a simple linear cavity MBRFL with a single Raman pump wavelength and employed large effective area fiber (LEAF) with the aim of the S-OSNR enhancement. Other report that accomplished a MBRFL with a double-pass structure and are able to produce a comb fiber laser with more than a few hundred of Stokes lines with 10 GHz spacing is also introduced by [29]. Despite these advantages, the main drawbacks associated with these lasers are their lower average output power and the non-uniformed Brillouin combs. Current research performed by Wang et al. with the aim of enhancing the flatness of the Brillouin Stokes lines utilizing only a single Raman pump [30]. Although, over 500 Stokes lines have been produced across 40 nm bandwidth, it suffers from very low S-OSNR of 12.5 dB and low output power. This is the highest number of channels acquired from a single Raman pump source reported until now. All of the aforementioned reported assessments are designed to attain multiple wavelengths with single wavelength spacing (10 GHz). Despite the research success, these techniques are not feasible as they are either very costly, or not well suited for practical application. In addition, due to the spectral broadening effect at higher pump power, the quality of Stokes lines in terms of optical signal-to-noise ratio (OSNR) is deteriorated [25]. As a result, together with the disadvantages existing in 10 GHz MBRFL the needs to explore alternative MBRFL sources have been increased.

1.2 Motivation

As discussed in the previous section, several MBRFL with 10 GHz wavelength spacing through different kinds of cavity configurations have been reported [17-18, 20-24, 27-30]. Nevertheless, these laser structures with low S-OSNR and narrow channel spacing is not practical for DWDM applications as it is difficult to demultiplex the channels at the receiver end. Thus, another design offering higher spectrum performances in terms of flatness, output peak power, and S-OSNR must be considered for MBRFL with 10 GHz spacing. However, the problem associated with the narrow wavelength spacing can be addressed by the development of MBRFL with wider spacing between BSL. In the earlier work [31], a MBRFL in a ring cavity with 22 GHz wavelength spacing is reported which is able to produce only 16 lines with a 11.7 dB S-OSNR. Although a MBRFL with double wavelength spacing has been realized, the exploitation of higher wavelength numbers with wider bandwidths and average excellent S-OSNR have been rarely demonstrated. Therefore, an alternative setup that improves MBRFL performance with double wavelength spacing (20 GHz) is also preferable. In this thesis, two different linear

cavity configurations are designed to achieve this objective. Moreover, in order to provide design flexibility and functionality, it is desirable to demonstrate a MBRFL source with an adjustable wavelength spacing (10 and 20 GHz spacing) with excellent performances to be more feasible for DWDM systems. Because the current DWDM systems have different channels spacing based on their specific applications. To achieve this, a new cavity design of MBRFL that utilizes a nonlinear amplifying fiber loop (NAFL) is proposed. In addition, further advancement in this cavity is performed as an alternative source for generation of MBRFL with 10 GHz spacing. The advantages of developing this configuration are due to its operation at very low Raman pump power (RPP) which permits the generation of multiple Brillouin Stokes signals (MBSS) with good performances.

1.3 Problem Statements

Even though MBRFL is an excellent approach to generate hundreds of Stokes line, it still has the following problems,

- i. Lower value of S-OSNR for both 10 and 20 GHz spacing.
- ii. Multi-frequency pump sources or multi-gain media requirement when high count, flattened multi-Stokes lines are needed.
- iii. There is no report on generating MBRFL with adjustable wavelength spacing.
- iv. Generation of a few MBSS with 10 GHz spacing and acceptable OSNR are achieved at the expense of high RPP and complex design.
- v. There is no study on generation of 20 GHz MBRFL with higher number of channels and good S-OSNR values reported.

In addition, an amplified spontaneous emission (ASE) noise and spectral broadening are two main drawbacks which impact on the MBRFL spectrum performances in terms of SLC and S-OSNR. In this doctoral research, all the aforementioned issues are addressed in the linear cavity MBRFL.

1.4 Objectives of This Research Work

Based on the problem statements stated in the earlier sections, there are some objectives needed to be realized and fulfilled in this research. The statements below are the objectives that are going to be achieved:

- i. To design a new MBRFL configuration with adjustable wavelength spacing (10 and 20 GHz spacing) with high number of channels and S-OSNR using only a single Raman pump source.
- ii. To design and develop a simple MBRFL with 10 GHz spacing with ability of generating MBSS at very low RPP.
- iii. To design and develop a simple MBRFL source with a 20 GHz spacing and enhance its spectral combs in terms of SLC, S-OSNR, SPP, and wavelength operation.

1.5 Scope of Research Work

Figure 1.1 shows the scope of works covered in this doctoral research. This work focuses on the MBRFL, which can be divided based on the wavelength spacing. The objective of this thesis is to propose and demonstrate simple configurations for MBRFL with single and double Brillouin frequency spacing shift. However, the main motivation is to design configurations for generating MBRFL with 20 GHz spacing. In this work, all configurations are based on linear cavity due to many advantages such as higher numbers of channels, wider multi-wavelength bandwidth, and higher S-OSNR in comparison with the ring cavity structures. A new structure for MBRFL with an adjustable 10 and 20 GHz spacing is realized by employing an enhanced NAFL design. Moreover, generation of more channels number with a reasonable S-OSNR at very low RPP has been successfully achieved by employing a mirror at the end of the NAFL design which dubbed as a nonlinear amplifying loop mirror (NALM). In addition, utilizing forward pumping (FWP) scheme and a new structure which involves various pump power distributions in forward-backward directions named as a bidirectional pumping (BiDP) scheme is also proposed. In all configurations, by varying the Brillouin pump (BP) power, BP wavelength, and RPP, their detail performances; namely SLC, wavelength operation, spectral combs and S-OSNRs are analyzed thoroughly. Finally, the output of the proposed architectures is compared to the prior works in terms of the SLC, S-OSNR, Stokes peak power (SPP), and RPP.

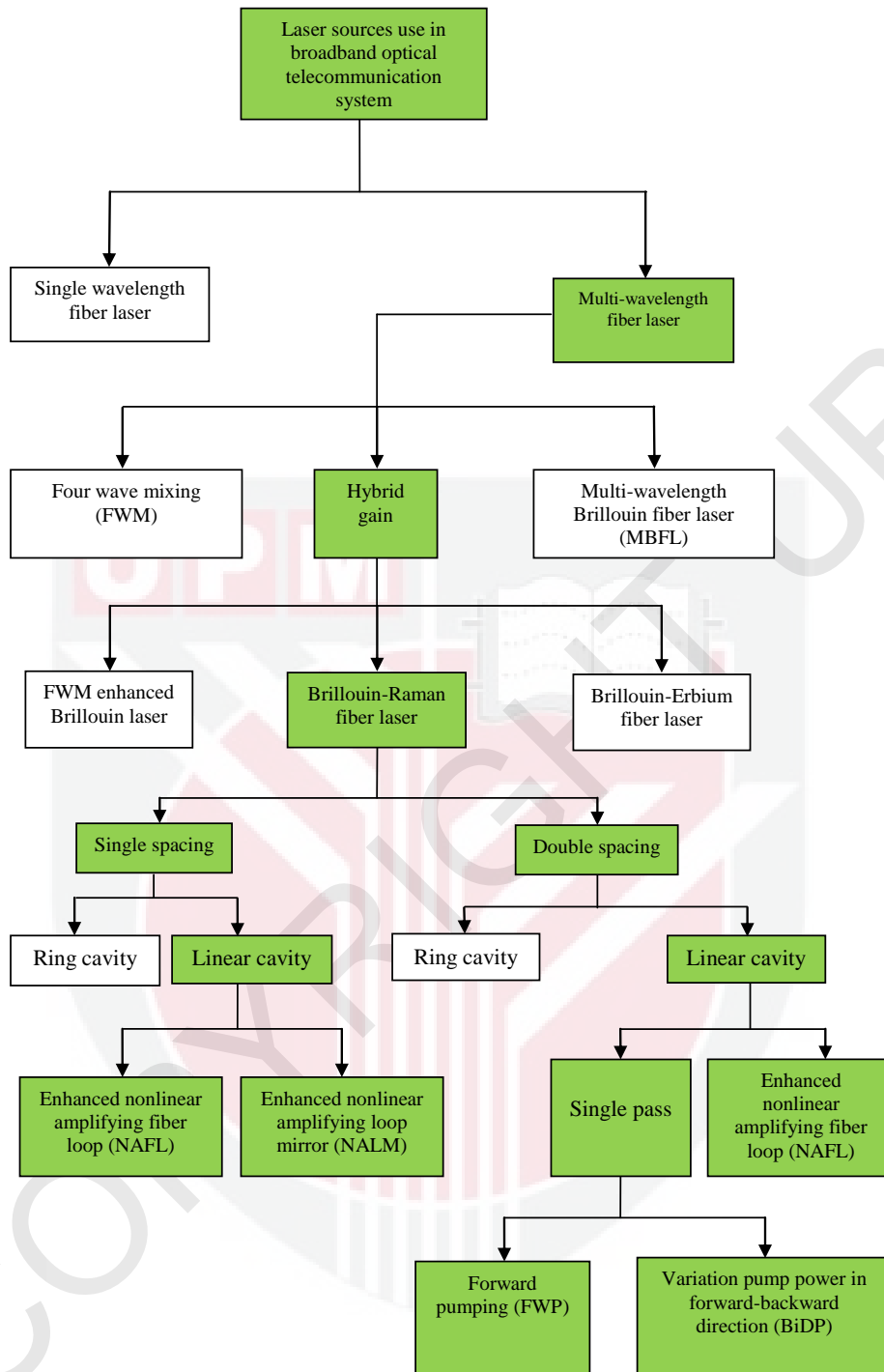


Figure 1.1: Scope of doctoral research.

1.6 Research Methodology

The methodology of this research is presented in Figure 1.2. Briefly, the thesis works are conducted through an experimental process that involves analysis of the optical parameters of generated MBSS as SLC, S-OSNR, SPP, and wavelength operation. Three main architectures are investigated which include enhanced NAFL and NALM designs in Chapter 3 and FWP-MBRFL, and BiDP-MBRFL in Chapter

4. In Chapter 3, a new design of NAFL with different set of couplers is demonstrated to achieve adjustable 10 and 20 GHz spacing operation. To realize this, a theoretical analysis is developed first which agrees well with the experimental results. By proper adjustment of coupling ratios, and optimization of laser parameters, MBRFL with 10 and 20 GHz spacing is satisfied with good characteristics. By employing a mirror at the one end of this configuration that dubbed as a NALM, multiple channels with 10 GHz spacing and a reasonable S-OSNR at very low RPP has been successfully accomplished. In Chapter 4, a simple linear cavity configuration through FWP scheme is arranged by employing 7.2 and 11 km DCFs in addition to a 30 cm Bismuth oxide erbium-doped fiber (Bi-EDF). This is done to achieve MBRFL with 20 GHz spacing with good lasing characteristics. Although 20 GHz spacing MBSS with good features is achieved, to enhance the lasing combs characteristics in terms of SLC, S-OSNR, SPP, and wavelength operation a new configuration of BiDP that implements a variable pumping scheme in backward and forward directions is also demonstrated. This scheme offers MBRFL with 20 GHz spacing and excellent performance. For all configurations, the effect of different input parameters including BP power, BP wavelength, and RPP on output spectra are studied experimentally. The trends of the Raman gain profile before launching the BP signal into the cavity are analyzed as well. For all configurations, the SLC and S-OSNR are measured when the Brillouin pump wavelength is selected at 1555 nm, while the RPP is varied from 800 mW to 1000 mW. In addition, the optical features of generated laser comb spectrum such as SLC are investigated when the BP power is varied from -2.6 to 5 dBm when the RPP is varied from 800 to 1000 mW. The wavelength operation is also investigated for all structures. The RPP is optimized to produce a flat amplitude MBRFL comprising maximum number of channels with high S-OSNR. Consequently, the outputs of each proposed configurations are measured by optical spectrum analyser (OSA). It is noted that the threshold of first Brillouin Stokes line is measured for all configurations when the RPP, BP power and BP wavelength are set at 1000 mW, 5 dBm and 1555 nm respectively. Finally, after analyzing experimental results from all configurations, the results that meet the thesis objectives are considered.

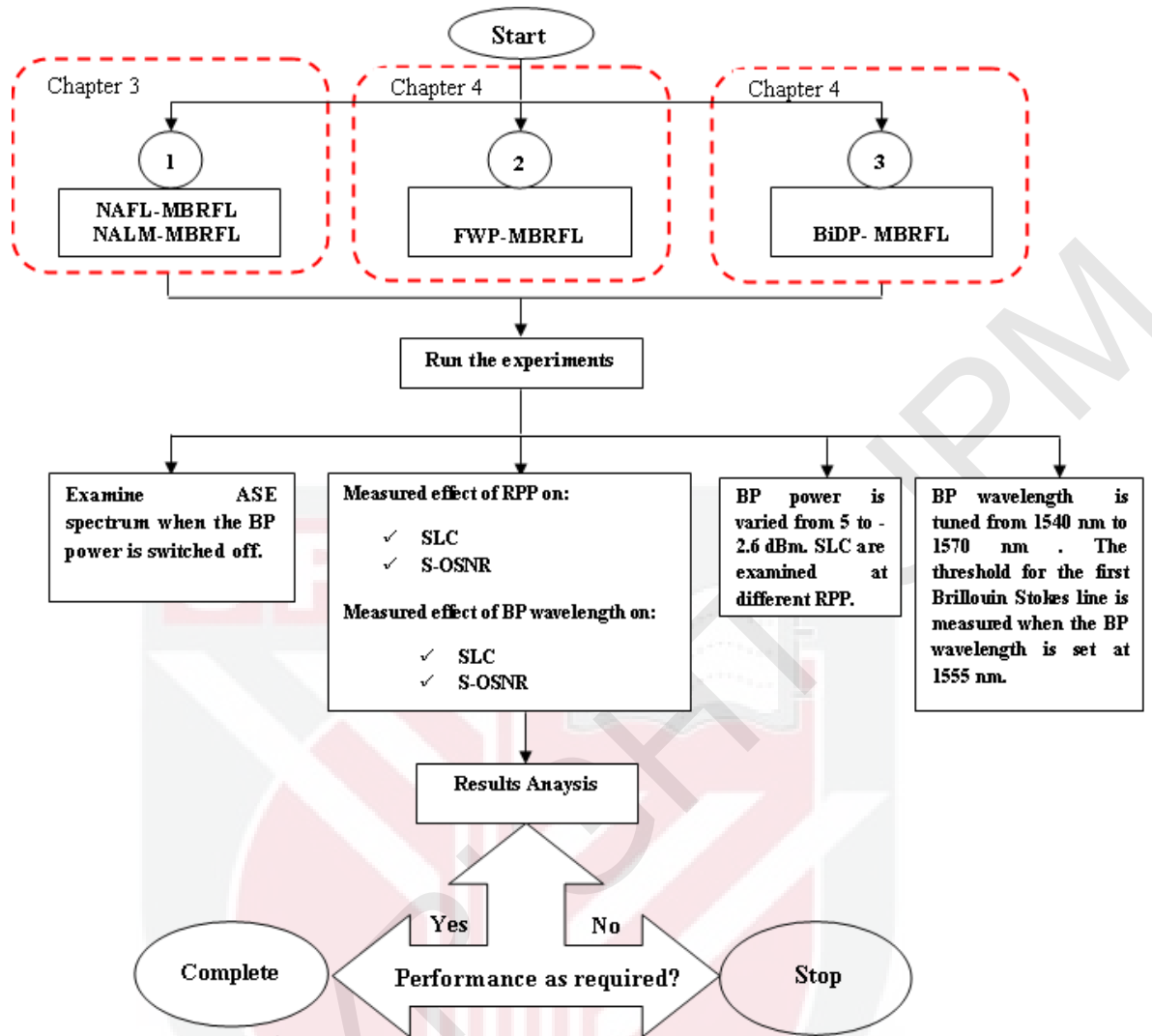


Figure 1.2: Research methodology flow-chart.

1.7 Thesis Overview

This thesis comprehensively studies the performance parameters of three proposed linear MBRFL sources, which employs dispersion compensating fiber (DCF) as the Brillouin-Raman gain medium. In general, this thesis consists of five chapters. Chapter 1, which is this current chapter, gives a general introduction of the topics and defines the context of the work.

Chapter 2 introduces an overview background on the basic concepts of nonlinear fiber optics effects and explains the theoretical backgrounds of nonlinear optical loop mirror (NOLM) and NALM. Moreover, principle operation of MBRFL generation and review of previous works on MBRFL generation is briefly discussed at the end of this chapter.

Chapter 3 proposes new configuration of NAFL for generating MBRFL with adjustable wavelength spacing. It started with the theoretical analysis of the NALM.

Afterward, experimental results are explained where good agreement is found with the theoretical results. The spectral characteristics of this cavity at optimized coupling ratios are studied thoroughly. In addition, by employing a mirror at one end of the NAFL design, generating a high number of lasing lines with a reasonable S-OSNR at very low RPP has been successfully satisfied.

Chapter 4 is devoted to the generation of MBRFL with 20 GHz spacing which includes two linear cavities through FWP and BiDP schemes. The setup implemented via FWP scheme arranged with different DCF lengths in addition to a 30 cm Bi-EDF. The influences of varying several parameters such as RPP, BP power, and BP wavelength on spectra features of all cavity arrangements are studied thoroughly. In order to enhance the characteristics of MBSS in terms of SLC, SPP, and wavelength operation, a simple configuration by employing various coupling ratios is constructed to provide different pump power distributions along the fiber longitudinal structure. By optimization pumping ratios, and BP characteristics, the lasing characteristics are improved. This scheme strongly offers a few advantages specially enhanced feasibility and simplicity due to the utilization of only one RPU.

The finding of this work is summarized and concluded in Chapter 5. The performances of the proposed configurations in contrast to each other and prior works are detailed in this chapter. Moreover, it includes the contribution of this thesis and the recommendation for further research work is also presented in this chapter.

REFERENCES

- [1] M. Yamada, "Overview of wideband optical fiber amplification technologies," *NTT Tech. Rev.*, vol. 2, pp. 34-37, 2004.
- [2] J. Hecht, "The First Half-Century of Laser Development," *Laser Tech.*, vol. 7, pp. 20-25, 2010.
- [3] J. Geng, *et al.*, "Highly stable low-noise Brillouin fiber laser with ultranarrow spectral linewidth," *IEEE Photon. Technol. Lett.*, vol. 18, pp. 1813-1815, 2006.
- [4] R. Parvizi, *et al.*, "Multi-wavelength Brillouin fiber laser using dual-cavity configuration," *Laser Phys.*, vol. 21, pp. 205-209, 2011.
- [5] Q. Mao and J. W. Y. Lit, "Switchable multi-wavelength erbium-doped fiber laser with cascaded fiber grating cavities," *IEEE Photon. Technol. Lett.*, vol. 14, pp. 612-614, 2002.
- [6] S. W. Harun, *et al.*, "Multi-wavelength erbium-doped fiber laser assisted by four wave mixing effect," *Laser Phys. Lett.*, vol. 6, pp. 813-815, 2009.
- [7] Y.-G. Han, *et al.*, "Multi-wavelength Raman fiber-ring laser based on tunable cascaded long-period fiber gratings," *IEEE Photon. Technol. Lett.*, vol. 15, pp. 383-385, 2003.
- [8] A. K. Abeeluck, *et al.*, "High-power supercontinuum generation in highly nonlinear, dispersion-shifted fibers by use of a continuous-wave Raman fiber laser," *Opt. Lett.*, vol. 29, pp. 2163-2165, 2004.
- [9] W. Guan and J. R. Marciante, "Dual-frequency operation in a short-cavity ytterbium-doped fiber laser," *IEEE Photon. Technol. Lett.*, vol. 19, pp. 261-263, 2007.
- [10] Z. Zhang, *et al.*, "Tunable self-seeded multi-wavelength Brillouin-erbium fiber laser with enhanced power efficiency," *Opt. Express*, vol. 15, pp. 9731-9736, 2007.
- [11] Y. J. Song, *et al.*, "Tunable multi-wavelength Brillouin-erbium fiber laser with a polarization-maintaining fiber Sagnac loop filter," *IEEE Photon. Technol. Lett.*, vol. 16, pp. 2015-2017, 2004.
- [12] M. H. Al-Mansoori and M. A. Mahdi, "Tunable range enhancement of Brillouin-erbium fiber laser utilizing Brillouin pump preamplification technique," *Opt. Express*, vol. 16, pp. 7649-7654, 2008.
- [13] M. H. Al-Mansoori and M. A. Mahdi, "Multi-wavelength L-band Brillouin-Erbium comb fiber laser utilizing nonlinear amplifying loop mirror," *J. Lightwave Technol.*, vol. 27, pp. 5038-5044, 2009.
- [14] Y. G. Shee, *et al.*, "Multi-wavelength Brillouin-erbium fiber laser with double-Brillouin-frequency spacing," *Opt. Express*, vol. 19, pp. 1699-1706, 2011.
- [15] M. Ajiya, *et al.*, "Broadly tunable multiple wavelength Brillouin fiber laser exploiting erbium amplification," *J. Opt. Soc. Am. B.*, vol. 26, pp. 1789-1794, 2009.
- [16] Y. J. Song, *et al.*, "Self-seeded multi-wavelength Brillouin-erbium fiber laser," *Opt. Lett.*, vol. 30, pp. 486-488, 2005.
- [17] B. Min, *et al.*, "Flat amplitude equal spacing 798-channel Rayleigh-assisted Brillouin-Raman multi-wavelength comb generation in dispersion

- compensating fiber," *IEEE Photon. Technol. Lett.*, vol. 13, pp. 1352-1354, 2001.
- [18] K.-D. Park, *et al.*, "Dynamics of cascaded Brillouin-Rayleigh scattering in a distributed fiber Raman amplifier," *Opt. Lett.*, vol. 27, pp. 155-157, 2002.
- [19] K.-d. Park, *et al.*, "Threshold features of a Brillouin Stokes comb generated in a distributed fiber Raman amplifier," *Opt. Lett.*, vol. 28, pp. 1311-1313, 2003.
- [20] Y.-g. Liu, *et al.*, "Stable room-temperature multi-wavelength lasing oscillations in a Brillouin-Raman fiber ring laser," *Opt. Commun.*, vol. 281, pp. 5400-5404, 2008.
- [21] J. W. Lou, *et al.*, "Brillouin fibre laser enhanced by Raman amplification," *Electron. Lett.*, vol. 40, pp. 1044-1046, 2004.
- [22] A. K. Zamzuri, *et al.*, "Brillouin-Raman comb fiber laser with cooperative Rayleigh scattering in a linear cavity," *Opt. Lett.*, vol. 31, pp. 918-920, 2006.
- [23] A. K. Zamzuri, *et al.*, "Flat amplitude multi-wavelength Brillouin-Raman comb fiber laser in Rayleigh-scattering-enhanced linear cavity," *Opt. Express*, vol. 15, pp. 3000-3005, 2007.
- [24] A. K. Zamzuri, *et al.*, "Contribution of Rayleigh scattering on Brillouin comb line generation in Raman fiber laser," *Appl. Opt.*, vol. 49, pp. 3506-3510, 2010.
- [25] A. K. Zamzuri, *et al.*, "OSNR variation of multiple laser lines in Brillouin-Raman fiber laser," *Opt. Express*, vol. 17, pp. 16904-16910, 2009.
- [26] A. K. Zamzuri, *et al.*, "Spectral variation in Brillouin-Raman fiber laser," in *Communications and Photonics Conference and Exhibition (ACP) 2009*, pp. 1-2.
- [27] H. Wu, *et al.*, "Flat amplitude multi-wavelength Brillouin-Raman random fiber laser with a half-open cavity," *Appl. Phys. B.*, vol. 112, pp. 467-471, 2013.
- [28] R. Sonee Shargh, *et al.*, "OSNR enhancement utilizing large effective area fiber in a multi-wavelength Brillouin-Raman fiber laser," *Laser Phys. Lett.*, vol. 8, pp. 139-143, 2011.
- [29] R. S. Shargh, *et al.*, "Improvement of comb lines quality employing double-pass architecture in Brillouin-Raman laser," *Laser Phys. Lett.*, vol. 8, pp. 823-827, 2011.
- [30] Z. Wang, *et al.*, "Broadband flat-amplitude multi-wavelength Brillouin-Raman fiber laser with spectral reshaping by Rayleigh scattering," *Opt. Express*, vol. 21, pp. 29358-29363, 2013.
- [31] N. A. M. A. Hambali, *et al.*, "Multi-wavelength Brillouin-Raman ring-cavity fiber laser with 22-GHz spacing," *Laser Phys.*, vol. 21, pp. 1656-1660, 2011.
- [32] M. F. Ferreira, *Nonlinear effects in optical fibers* vol. 2: John Wiley & Sons, 2011.
- [33] Q. Lin, *et al.*, "Nonlinear optical phenomena in silicon waveguides: modeling and applications," *Opt. Express*, vol. 15, pp. 16604-16644, 2007.
- [34] J. Hecht and L. Long, *Understanding fiber optics*: Prentice Hall Upper Saddle River, NJ, 2002.
- [35] G. P. Agrawal, *Nonlinear fiber optics*: Academic press, 2007.
- [36] Y.-R. Shen, "The principles of nonlinear optics," *New York, Wiley-Interscience*, 1984.

- [37] E. L. Buckland and R. W. Boyd, "Electrostrictive contribution to the intensity-dependent refractive index of optical fibers," *Opt. Lett.*, vol. 21, pp. 1117-1119, 1996.
- [38] N. J. Doran and D. Wood, "Nonlinear-optical loop mirror," *Opt. Lett.*, vol. 13, pp. 56-58, 1988.
- [39] G. New, *Introduction to Nonlinear Optics*: Cambridge University Press, 2011.
- [40] R. W. Boyd, *Nonlinear optics*: Academic press, 2003.
- [41] B. Batagelj, *et al.*, "Use of four-wave mixing in optical fibers for applications in transparent optical networks," in *Proceedings of 6th International Conference on Transparent Optical Networks*, 2004, pp. 215-220.
- [42] I. Neokosmidis, *et al.*, "New techniques for the suppression of the four-wave mixing-induced distortion in nonzero dispersion fiber WDM systems," *J. Lightwave Technol.*, vol. 23, pp. 1137 - 1144, 2005.
- [43] R. Tkach, *et al.*, "Four-photon mixing and high-speed WDM systems," *J. Lightwave Technol.*, vol. 13, pp. 841-849, 1995.
- [44] S. A. Babin, *et al.*, "Four-wave-mixing-induced turbulent spectral broadening in a long Raman fiber laser," *J. Opt. Soc. Am. B.*, vol. 24, pp. 1729-1738, 2007.
- [45] J. Hagen, *et al.*, "Numerical modeling of intracavity spectral broadening of Raman fiber lasers," *IEEE Photon. Technol. Lett.*, vol. 19, pp. 1759-1761, 2007.
- [46] S. P. Singh and N. Singh, "Nonlinear effects in optical fibers: Origin, management and applications," *Prog. Electromagn Res.*, vol. 73, pp. 249-275, 2007.
- [47] E. P. Ippen and R. H. Stolen, "Stimulated Brillouin scattering in optical fibers," *Appl. Phys. Lett.*, vol. 21, pp. 539-541, 1972.
- [48] S. W. Harun, *et al.*, "Multi-wavelength source using a Brillouin fiber laser," *J. Nonlinear Opt. Phys.*, vol. 17, pp. 199-203, 2008.
- [49] P. T. Rakich, *et al.*, "Giant enhancement of stimulated Brillouin scattering in the subwavelength limit," *Phys. Rev. X.*, vol. 2, pp. 011008-, 2012.
- [50] K. Shiraki, *et al.*, "SBS threshold of a fiber with a Brillouin frequency shift distribution," *J. Lightwave Technol.*, vol. 14, pp. 50-57, 1996.
- [51] R. H. Stolen, *et al.*, "Raman oscillation in glass optical waveguide," *Appl. Phys. Lett.*, vol. 20, pp. 62-64, 1972.
- [52] C. Headley and G. Agrawal, *Raman amplification in fiber optical communication systems*: Academic Press, 2005.
- [53] S. Namiki, *et al.*, "Challenges of Raman amplification," *IEEE. Proc.*, vol. 94, pp. 1024-1035, 2006.
- [54] R. G. Smith, "Optical power handling capacity of low loss optical fibers as determined by stimulated Raman and Brillouin scattering," *Appl. Opt.*, vol. 11, pp. 2489-2494, 1972.
- [55] J. Bromage, *et al.*, "Raman Amplifiers and Oscillators in Telecommunications," *MN Islam, Springer Verlag*, 2003.
- [56] G. Agrawal, *Applications of nonlinear fiber optics*: Access Online via Elsevier, 2001.
- [57] B. Nelson, *et al.*, "All-optical Gbit/s switching using nonlinear optical loop mirror," *Electron. Lett.*, vol. 27, pp. 704-705, 1991.
- [58] M. E. Fermann, *et al.*, "Nonlinear amplifying loop mirror," *Opt. Lett.*, vol. 15, pp. 752-754, 1990.

- [59] D. J. Richardson, *et al.*, "Very low threshold Sagnac switch incorporating an erbium doped fibre amplifier," *Electron. Lett.*, vol. 26, pp. 1779-1781, 1990.
- [60] Y.-G. Han, *et al.*, "Multi-wavelength Raman-fiber-laser-based long-distance remote sensor for simultaneous measurement of strain and temperature," *Opt. Lett.*, vol. 30, pp. 1282-1284, 2005.
- [61] S. Pan and J. Yao, "Frequency-switchable microwave generation based on a dual-wavelength single-longitudinal-mode fiber laser incorporating a high-finesse ring filter," *Opt. Express*, vol. 17, pp. 12167-12173, 2009.
- [62] Y.-G. Han, *et al.*, "Wavelength-spacing tunable multiwavelength erbium-doped fiber laser based on four-wave mixing of dispersion-shifted fiber," *Opt. Lett.*, vol. 31, pp. 697-699, 2006.
- [63] X. Feng, *et al.*, "Stable and uniform multi-wavelength erbium-doped fiber laser using nonlinear polarization rotation," *Opt. Express*, vol. 14, pp. 8205-8210, 2006.
- [64] Z. Zhang, *et al.*, "Multi-wavelength fiber laser with fine adjustment, based on nonlinear polarization rotation and birefringence fiber filter," *Opt. Lett.*, vol. 33, pp. 324-326, 2008.
- [65] L. Zhan, *et al.*, "160-line multi-wavelength generation of linear-cavity self-seeded Brillouin-erbium fiber laser," *Opt. Express*, vol. 14, pp. 10233-10238, 2006.
- [66] A. Loayssa, *et al.*, "Applications of optical carrier Brillouin processing to microwave photonics," *Opt. Fiber Technol.*, vol. 8, pp. 24-42, 2002.
- [67] Z. Y. Liu, *et al.*, "Tunable multi-wavelength erbium-doped fiber laser with a polarization-maintaining photonic crystal fiber Sagnac loop filter," *Laser Phys. Lett.*, vol. 5, pp. 446-448, 2008.
- [68] S. Pan, *et al.*, "Multi-wavelength erbium-doped fiber laser based on inhomogeneous loss mechanism by use of a highly nonlinear fiber and a Fabry-Perot filter," *Opt. Express*, vol. 14, pp. 1113-1118, 2006.
- [69] J. Tang, *et al.*, "Tunable multi-wavelength generation based on Brillouin-erbium comb fiber laser assisted by multiple four-wave mixing processes," *Opt. Express*, vol. 19, pp. 14682-14689, 2011.
- [70] M. R. Shirazi, *et al.*, "Multi-wavelength Brillouin-Raman fiber laser generation assisted by multiple four-wave mixing processes in a ring cavity," *Laser Phys.*, vol. 23, pp. 075108-075116, 2013.
- [71] N. Ahmad Hambali, *et al.*, "Singlewavelength ring-cavity Brillouin-Raman fiber laser," *Laser Phys. Lett.*, vol. 7, pp. 454-457, 2010.
- [72] N. Ahmad Hambali, *et al.*, "L-band multi-wavelength Brillouin-Raman fiber laser utilizing the reverse-S-shaped section," *J. Nonlinear Opt. Phys. Mat.*, vol. 23, pp. 1450026 -1450036, 2014.
- [73] Z. Zhang, *et al.*, "Research of distributed optical fiber Raman gain amplifier," in *Asia-Pacific Optical and Wireless Communications Conference and Exhibit*, 2001, pp. 54-56.
- [74] L. L. Grüner-Nielsen, *et al.*, "Dispersion compensating fibers," *Opt. Fiber Technol.*, vol. 6, pp. 164-180, 2000.
- [75] A. K. Abass, *et al.*, "Characteristics of multi-wavelength L-band Brillouin-Raman fiber laser under forward and backward pumped environment," *Appl. Opt.*, vol. 52, pp. 3764-3769, 2013.
- [76] H.-P. Gong and Z.-X. Zhang, "The Amplification Effect on Rayleigh Scattering and SBS in 25Km distributed fiber Raman Amplifier," in *Optical Fiber Sensors Conference*, 2008, pp. 1-4.

- [77] M. Pang, *et al.*, "Rayleigh scattering-assisted narrow linewidth Brillouin lasing in cascaded fiber," *Opt. Lett.*, vol. 37, pp. 3129-3131, 2012.
- [78] M. Mehendale, *et al.*, "Effect of Raman amplification on stimulated Brillouin scattering threshold in dispersion compensating fibres," *Electron. Lett.*, vol. 38, pp. 268-269, 2002.
- [79] M. R. Shirazi, *et al.*, "Effects of different Raman pumping schemes on stimulated Brillouin scattering in a linear cavity," *Appl. Opt.*, vol. 47, pp. 3088-3091, 2008.
- [80] A. Kobayakov, *et al.*, "Stimulated Brillouin scattering in Raman-pumped fibers: A theoretical approach," *J. Lightwave Technol.*, vol. 20, pp. 1635-1643, 2002.
- [81] S. P. N. Cani, *et al.*, "Raman amplifier performance of dispersion compensating fibers," in *Microwave and Optoelectronics Conference 2003*, pp. 553-558.
- [82] M. Mehendale, *et al.*, "Stimulated Brillouin scattering in Raman-amplified dispersion compensating fibers," in *Optical Fiber Communication Conference and Exhibit, OFC*, 2002, pp. 560-561.
- [83] S. Boscolo, *et al.*, "Design of Raman-based nonlinear loop mirror for all-optical 2R regeneration of differential phase-shift-keying transmission," *IEEE J. Quantum Electron.*, vol. 42, pp. 619-624, 2006.
- [84] J. Bromage, "Raman amplification for fiber communications systems," *J. Lightwave Technol.*, vol. 22, pp. 79-, 2004.
- [85] Y. K. Kwok, *Applied complex variables for scientists and engineers*, Taylor & Francis ed.: Cambridge University Press, 2002.
- [86] H. S. Kasana, *Complex variables: theory and applications*: PHI Learning Pvt. Ltd., 2005.
- [87] S. G. Krantz, *Function theory of several complex variables*: Wiley New York, 1982.
- [88] R. S. Shargh, *et al.*, "Effect of Raman pump direction on conventional multi-wavelength Brillouin-Raman fiber laser," in *3rd International Conference on Photonics (ICP)*, 2012, pp. 184-186.
- [89] S. A. Babin, *et al.*, "Turbulence-induced square-root broadening of the Raman fiber laser output spectrum," *Opt. Lett.*, vol. 33, pp. 633-635, 2008.
- [90] S. A. Babin, *et al.*, "Turbulent broadening of optical spectra in ultralong Raman fiber lasers," *Phys. Rev. A.*, vol. 77, pp. 0338031-0338035, 2008.
- [91] S. Ohara and Y. Kuroiwa, "Highly ytterbium-doped bismuth-oxide-based fiber," *Opt. Express*, vol. 17, pp. 14104-14108, 2009.
- [92] H. Ahmad, *et al.*, "Bismuth-based erbium-doped fiber as a gain medium for L-band amplification and Brillouin fiber laser," *Laser Phys.*, vol. 20, pp. 716-719, 2010.
- [93] Y. Fujimoto and M. Nakatsuka, "Optical amplification in bismuth-doped silica glass," *Appl. Phys. Lett.*, vol. 82, pp. 3325-3326, 2003.
- [94] Z. Tong, *et al.*, "Theoretical investigation and optimization of bi-directionally pumped broadband fiber Raman amplifiers," *Opt. Commun.*, vol. 217, pp. 401-413, 2003.
- [95] J. C. Bouteiller, *et al.*, "Dual-order Raman pump," *IEEE Photon. Technol. Lett.*, vol. 15, pp. 212-214, 2003.
- [96] J. Bromage, *et al.*, "WDM transmission over multiple long spans with bidirectional Raman pumping," *J. Lightwave Technol.*, vol. 22, pp. 225-232, 2004.